A Statistical Analysis of the Response of Tall Buildings to Recorded and Simulated Ground Motions

N. Jayaram & N. Shome
Risk Management Solutions Inc., Newark, CA, USA

SUMMARY:
Performance based earthquake engineering often involves dynamic structural analysis of buildings using a set of input ground motions. This manuscript describes statistical analyses performed to evaluate the similarity of the response of tall buildings to comparable recorded and simulated ground motions. Structural response measures of a 40 story steel moment frame building designed based on the 2006 IBC are estimated under comparable sets of 40 recorded and simulated ground motions selected from the NGA database and the 2009 broadband Loma Prieta simulations by Dr. Rob Graves. Commonly used response measures such as peak story drift ratio, peak floor acceleration, residual drift ratio and beam plastic rotation are considered. Hypothesis testing is used to compare and contrast the response measures obtained using the selected recorded and simulated ground motions. Overall, this study provides a statistical basis to test simulated ground motions and identify applications where simulated ground motions can be used.

Simulated ground motions, tall buildings, hypothesis testing, structural response, ground motion selection

1. INTRODUCTION

Performance based earthquake engineering (PBEE) often involves dynamic structural analysis of buildings using a set of input ground motions whose response spectra match a target response spectrum. On occasions where recorded ground motions are not sufficient, simulated ground motions are sometimes used to complete the ground-motion set (e.g., PEER Tall Building Initiative, Moehle et al., 2011). The mechanics of ground-motion simulation have advanced considerably in the past decade, but simulations are not yet widely used by the engineering community due to concerns regarding the validity of building response assessments carried out using simulated ground motions. In order to allay these concerns, researchers have recently started focusing on developing approaches to compare recorded and simulated ground motions and evaluating the applicability of simulations to PBEE (e.g., Luco and Somerville, 2011).

In the current study, statistical analyses are performed to evaluate the level of similarity between the response of tall buildings to comparable recorded and simulated ground motions. Structural response measures of a 40 story steel moment frame building designed based on the 2006 IBC are estimated under 40 recorded and simulated ground motions selected from the Pacific Earthquake Engineering Research (PEER) Next Generation Attenuation (NGA) database (Chiou et al., 2008) and the 2009 broadband Loma Prieta simulations by Dr. Rob Graves (Aagaard et al., 2008), respectively. The ground motions are selected such that the mean and variance of their spectra match a pre-specified target mean and the variance. In order to ensure that the recorded and simulated ground motions are comparable, it is made sure that for each recorded ground motion, a simulated ground motion is selected so that the response spectra of both ground motions match. Additional constraints are imposed on the magnitudes, distances and the durations corresponding to the selected ground motions. The response measures considered are peak story drift ratio, peak floor acceleration and residual drift ratio - measures that are commonly used to assess building performance and design buildings.

Hypothesis testing is then used to compare and contrast the response measures obtained using the selected recorded and simulated ground motions.

2. BUILDING MODEL

In this study, a 40-story steel moment resisting frame (SMRF) building designed based on the 2006 IBC is used as the illustrative tall building. Simplified analytical models are used in this study, given the numerous uncertainties in architectural and structural design decisions. Torsional effects and biaxial effects in columns are neglected, and therefore, only two-dimensional analytical models are employed. All moment-resisting bays are lumped into a single-bay moment frame, and P-Delta effects that are tributary to the gravity system are accounted for using a leaning column. Overturning moment effects on strength (column axial forces) and stiffness (flexural mode of displacement) are simulated by adjusting the bay width of the single bay frame. Such a model greatly reduces the computational effort and often facilitates interpretation of global results.

The analytical models of the tall buildings are analyzed using the OpenSees platform (http://opensees.berkeley.edu). The models for the flexural behavior of steel components are based on the point hinge concept and utilize a backbone curve that is discussed in detail in the PEER/ATC-72-1 report (ATC-72, 2010). The deterioration parameters of the backbone curve are based on regression equations developed using experimental results (Lignos and Krawinkler, 2009), and are functions of the geometric section and material properties that control deterioration in strength and stiffness due to local and lateral torsional buckling. Modeling deterioration in component properties is important particularly at large ground-motion intensities where dynamic instability (collapse) is approached. In all response history analyses, a Rayleigh damping of 2.5% is assigned at the first mode period T_1 and at $T = 0.2T_1$. It is seen that the responses estimated using this simplified model are very similar to those obtained using a more refined analytical model in which all moment frame bays were modeled individually, which serves as a validation of the single-bay frame model used in this study. Additional design and testing details are provided by Jayaram et al., 2012.

3. GROUND-MOTION SELECTION

The building model described above is analyzed under sets of 40 recorded and simulated ground motions. The recorded ground motions are chosen from the PEER NGA database, while the simulated ground motions are chosen from Dr. Rob Graves' Loma Prieta simulations. The building is assumed to be located at the Civic Center in Los Angeles, and the ground motions are chosen to be representative of the ground motions at that location. The basis for selecting these ground motions can be understood from the form of the ground-motion prediction equations given below:

$$lnS_a(T) = \overline{lnS_a(T)} + \sigma_{lnS_a(T)}\epsilon(T) \tag{3.1}$$

where $\overline{lnS_a(T)}$ denotes the predicted (by the ground-motion model) mean logarithmic spectral acceleration at period T, which depends on parameters such as magnitude, distance and local-site conditions; $\epsilon(T)$ denotes the normalized (total) residual and $\sigma_{lnS_a(T)}$ denotes the logarithmic standard deviation that is estimated as part of the ground-motion model. The 2,475yr return period spectral acceleration at the building's fundamental period (6.3s) is approximately 0.07g. The contribution of various earthquake events (magnitudes, faults) to this hazard level can be estimated using hazard deaggregation (USGS, 2008), which is a process that provides the likelihood that this hazard level is caused by an event with a certain magnitude, occurring on a certain rupture, with a certain residual value (M-R-ε combination). For the 2,475yr hazard at the Los Angeles Civic Center, the mean M, R, ε(6.3s) values are 6.5, 5km and 1. Therefore, the ground motions are selected such that their spectra have a mean and variance that would be expected for this scenario event. It is to be noted that for the purpose of this work, the choice of the target spectrum is not critical as long as both the recorded and the simulated ground motions have similar properties (as described subsequently).

3.1. Estimation of the target mean and variance

Traditionally, site and structure-specific ground-motion selection methods often involve selecting a set of ground motions whose response spectra match a site-specific target median response spectrum without any consideration of the inherent variance in the response spectrum. Estimates of structural response obtained using the ground motions selected only based on the median values will show smaller than 'actual' variance. Therefore, this work focuses on capturing both the mean spectrum as well as the variability in the spectrum. The target mean and variance corresponding to the M-R-ε(6.3s) scenario is estimated using the conditional mean spectrum (CMS) method (Baker, 2005). The fundamental concept involved in the CMS is that the response spectrum is a collection of spectral accelerations at various periods (T_js) that can reasonably be assumed to follow a joint lognormal distribution (Jayaram and Baker, 2008). This spectrum has a mean value at all the periods for a given scenario event, but also has significant variability around it. This is because although the scenario defines the value of ε to be 1.0 at 6.3s, ε can take a range of values at any other period, as explained subsequently. The following steps describe the calculation of the mean and the variance of the (logarithmic) response spectrum (i.e., [$\ln S_a(T_1)$, $\ln S_a(T_2)$,…, $\ln S_a(T_n)$]):

Step1: For all the T_is of interest (in this study, 20 periods between 0 and 10s are used), compute the unconditional mean and standard deviation of the logarithmic response spectrum using M and R. In other words, compute $\overline{lnS_a(T_i)}$ and $\sigma_{lnS_a(T_i)}$.

Step 2: Compute the mean of the response spectrum conditioned on $\varepsilon(T_0 = 6.3\text{s}) = 1$ (as obtained from deaggregation). The conditional mean matrix (μ) is as follows:

$$\mu = \begin{bmatrix} \mu_{lnS_a(T_1)} + \rho(T_1, T_0)\epsilon(T_0)\sigma_{lnS_a(T_1)} \\ \mu_{lnS_a(T_2)} + \rho(T_2, T_0)\epsilon(T_0)\sigma_{lnS_a(T_2)} \\ . \\ . \\ \mu_{lnS_a(T_n)} + \rho(T_n, T_0)\epsilon(T_0)\sigma_{lnS_a(T_n)} \end{bmatrix} \tag{3.2}$$

where $\rho(T_i, T_0)$ is the correlation between $\varepsilon(T_i)$ and $\varepsilon(T_0)$ provided by, for instance, Baker and Jayaram (2008).

Step 3: Let Σ denote the covariance matrix of [$\ln S_a(T_a)$, $\ln S_a(T_b)$,…, $\ln S_a(T_n)$] conditioned on $\varepsilon(T_0 = 6.3\text{s}) = 1$. Let Σ_0 denote the unconditional covariance matrix of [$\ln S_a(T_a)$, $\ln S_a(T_b)$,…, $\ln S_a(T_n)$] and Σ_1 denote the covariance between [$\ln S_a(T_a)$, $\ln S_a(T_b)$,…, $\ln S_a(T_n)$] and $\ln S_a(T_0)$.

$$\Sigma_0 = \begin{bmatrix} \sigma^2_{\ln S_a(T_1)} & \rho(T_1, T_2)\sigma_{\ln S_a(T_1)}\sigma_{\ln S_a(T_2)} & \cdots & \rho(T_1, T_n)\sigma_{\ln S_a(T_1)}\sigma_{\ln S_a(T_n)} \\ \rho(T_2, T_1)\sigma_{\ln S_a(T_2)}\sigma_{\ln S_a(T_1)} & \sigma^2_{\ln S_a(T_2)} & \cdots & \rho(T_2, T_n)\sigma_{\ln S_a(T_2)}\sigma_{\ln S_a(T_n)} \\ \vdots & \vdots & \ddots & \vdots \\ \rho(T_n, T_1)\sigma_{\ln S_a(T_n)}\sigma_{\ln S_a(T_1)} & \rho(T_n, T_2)\sigma_{\ln S_a(T_n)}\sigma_{\ln S_a(T_2)} & \cdots & \sigma^2_{\ln S_a(T_n)} \end{bmatrix} \tag{3.3}$$

Σ can be computed as follows [14]:

$$\Sigma = \Sigma_0 - \frac{1}{\sigma^2_{lnS_a(T_0)}}\Sigma_1\Sigma_1' \tag{3.4}$$

where $\Sigma_1^{'}$ denotes the transpose of Σ_1.

The exponential of the target mean (Eqn. 3.2) and the variance (diagonals of the covariance matrix shown in Eqn. 4) for the target scenario of interest are shown in Fig. 3.1. The conditional variance is 0 at 6.3s because the value of ε at 6.3s is deterministically set to 1.0 in the chosen scenario based on hazard deaggregation as described earlier.

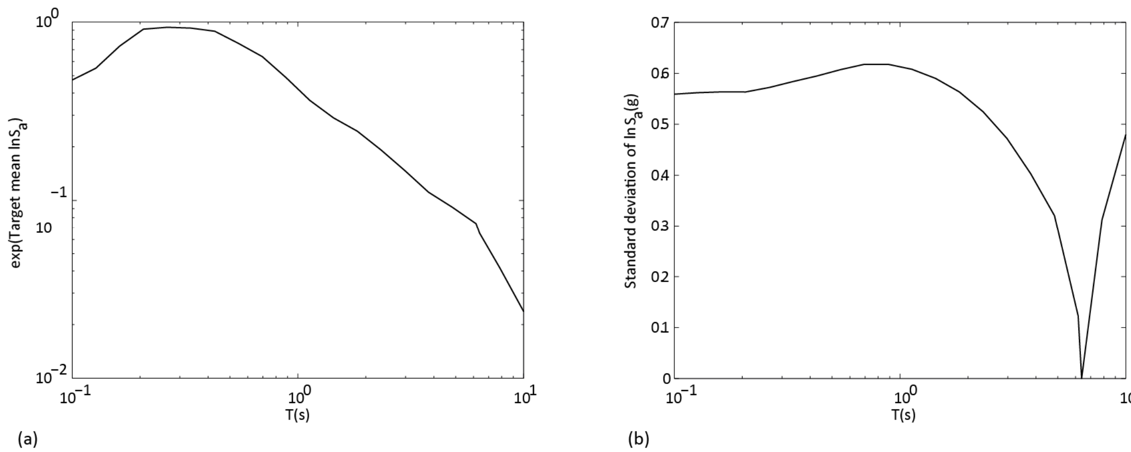

Figure 3.1. (a) Exponential of the target logarithmic mean spectrum, and (b) Target standard deviation of the logarithmic mean spectrum.

3.2. Ground-motion selection

Forty recorded and simulated ground motions are now selected such that their spectra mean and variance match the target values shown in Eqns. 3.2 and 3.4 respectively. This is done using the ground motion selection algorithm of Jayaram et al. (2011). The selection algorithm probabilistically generates multiple response spectra from a target distribution, and then selects ground motions whose response spectra individually match the simulated response spectra. Further in order to ensure compatibility between the recorded and simulated ground motions, for each recorded ground motion, a simulated ground motion is selected so that the response spectra of both ground motions match obtaining a comparable pair of records. Fig. 3.2 shows the response spectra of the selected recorded and simulated ground motions. Fig. 3.3 shows the comparison to the target mean and standard deviation. Irrespective of the match to the actual target (which is not critical), it is important to note that the mean and the standard deviation of the recorded and simulated ground-motion spectra are very similar to each other. Incidentally, Fig. 3.3 also shows correlations between logarithmic spectral accelerations at two different periods estimated using the recorded and the simulated ground motions. In addition to the mean and standard deviation, the correlations can also be noted to be similar between the two sets (slightly higher correlations are seen for the simulated set at short periods).

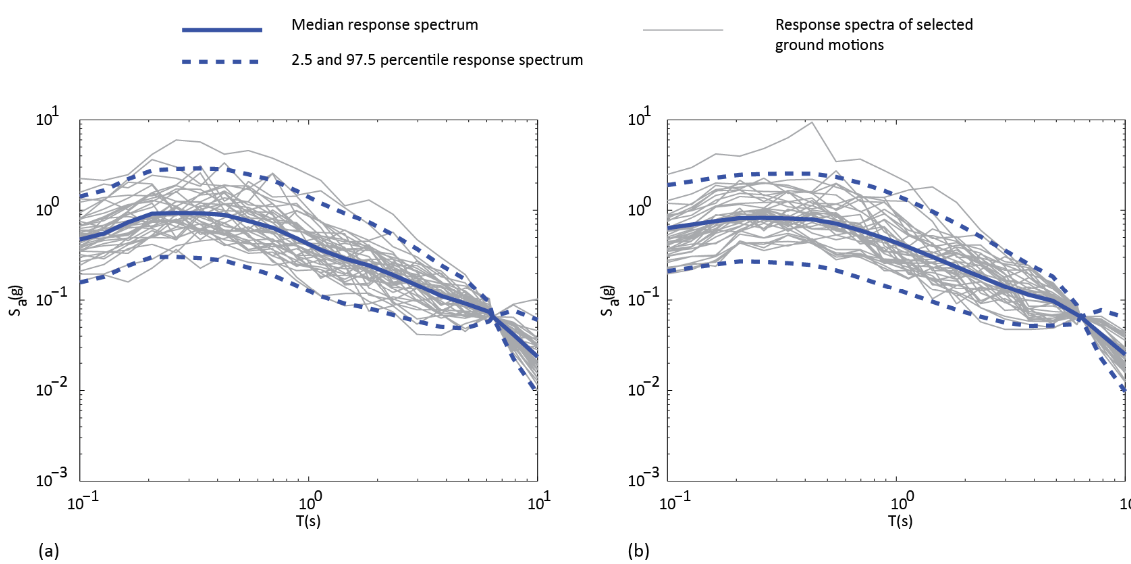

Figure 3.2. Response spectra of selected (a) recorded and (b) simulated ground motions.

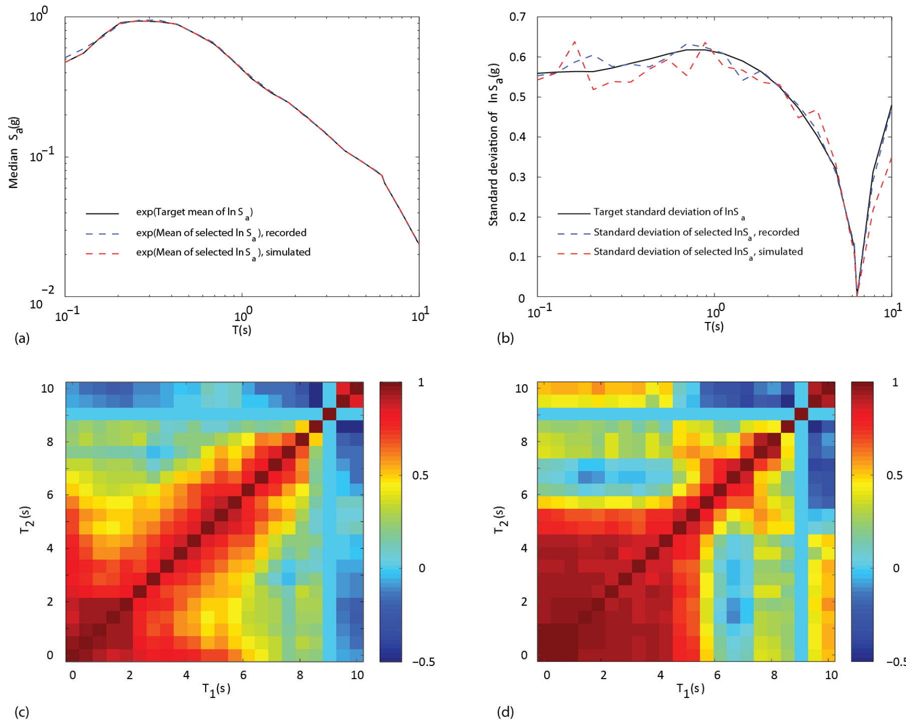

Figure 3.3. (a) Target and sample median spectrum, (b) Target and sample dispersion, and period-period log spectral acceleration correlation for the selected (c) recorded and (d) simulated ground motions.

4. HYPOTHESIS TESTING TO COMPARE RESPONSE MEASURES

In this study, hypothesis testing (e.g., Kutner et al. 2005) is used to identify whether the response measures estimated using the recorded ground motions are statistically significantly different from those estimated using simulated ground motions. Hypothesis testing helps identify whether the differences in the response measures are simply due to randomness associated with finite sample sizes or are inherent. Suppose we are interested in testing whether the mean peak floor accelerations (PFA) estimated using the recorded and the simulated ground motions are different, define the hypotheses of interest as follows:

Null Hypothesis: mean(PFA_{rec}) – mean(PFA_{sim}) = 0

Alternate Hypothesis: mean(PFA_{rec}) – mean(PFA_{sim}) ≠ 0

where PFA_{rec} and PFA_{sim} are the PFA values estimated using recorded and simulated ground motions respectively. The null hypothesis states that the true difference between the means of these two parameters equals zero, indicating that any difference in the estimates we observe using the selected ground motions is purely due to randomness associated with the finite sample size.

The null hypothesis can be rejected if the sample means estimated using the selected ground motions are significantly apart that the difference is unlikely to have been caused if their true means were the same. In other words, we reject the null hypothesis if the difference between the sample means exceeds a threshold value, estimated as follows:

Under the null hypothesis, the difference between the sample mean of PFA_{rec} (denoted $\overline{PFA}_{rec}$) and PFA_{sim} (denoted $\overline{PFA}_{sim}$) follows a Normal distribution with mean 0 and standard deviation $\hat{s}_{PFA}\sqrt{\frac{1}{n_{rec}}+\frac{1}{n_{sim}}}$, where $\hat{s}_{PFA}$ is the sample standard deviation of PFA (obtained as the pooled standard deviation of the recorded and the simulated ground-motion response results – the pooled estimate is used because it has a lower standard error), n_{rec} and n_{sim} are the number of recorded and simulated ground motions respectively. Typically, the null hypothesis is rejected when the estimated difference in the mean values falls outside the 2.5 and 97.5%iles of the above Normal distribution. In other words, the null hypothesis is rejected if:

$$\overline{PFA}_{rec} - \overline{PFA}_{sim} \notin \left[\pm 1.96\hat{s}_{PFA}\sqrt{\frac{1}{n_{rec}} + \frac{1}{n_{sim}}}\right] \tag{4.1}$$

$$\text{(or)}\ \overline{PFA}_{sim} \notin \left[\overline{PFA}_{rec} \pm 1.96\hat{s}_{PFA}\sqrt{\frac{1}{n_{rec}} + \frac{1}{n_{sim}}}\right]$$

An alternate approach to deriving the rejection region is the method of bootstrapping (Efron and Tibshirani, 1993), in which the 40 sample estimates of $PFA_{rec} - PFA_{sim}$ (corresponding to the 40 selected ground motions) are sampled with replacement several times to create new sets of 40 $PFA^{*}{}_{rec} - PFA^{*}{}_{sim}$ values. For every such set, the mean of the differences is computed and stored. The null hypothesis is rejected if the difference in the sample mean falls outside the 2.5 and the 97.5 percentiles of the resampled means of the differences. The bootstrap method, in theory, should produce the bounds shown in Eqn. 4.1 and hence, it is possible to just use Eqn. 4.1 while comparing the means. This bootstrap method is particularly advantageous for deriving the rejection region for data moments other than the mean such as standard deviations and correlations for which closed-form bounds are harder to derive.

The next section describes whether the hypothesis tests carried out in the current study resulted in the rejection of any of the null hypotheses, which would indicate that there are some fundamental differences in the response results estimated using comparable recorded and simulated ground motions.

5. RESULTS AND DISCUSSION

Fig. 5.1a shows the exponential mean peak (over time) logarithmic story drift ratios estimated using recorded and simulated ground motions. From this figure, it can be seen that the simulated ground motion values are reasonably within the boundaries of the rejection region derived based on Eqn. 4.1. Fig. 5.1b shows the standard deviations of the logarithmic story drift ratios along with the corresponding rejection region boundary. The results from the simulations are reasonably within the boundaries shown. In addition, Figs. 5.1c and 5.1d show the correlation between the PFAs from one story to another, as estimated using the recorded and the simulated ground motions respectively. The absolute mean correlation difference equals 0.12, while the bootstrap theoretical rejection threshold equals 0.24, indicating that the difference of 0.12 does not necessarily indicate that the recorded and simulated ground motions produce statistically significantly different correlations.

Figs. 5.2-5.4 show similar results for accelerations, residual drift ratios and beam plastic rotations. The absolute mean differences in the correlations between these EDPs and the corresponding rejection thresholds (shown within parenthesis) for PFA, residual drift and beam rotation are 0.07(0.11), 0.29(0.29) and 0.15(0.20) respectively. In general, while there are some differences between the results obtained using recorded and simulated ground motions, statistically significant differences are only seen for the mean residual drift ratios. While the differences are not significant for most of the parameters considered, additional work is necessary to identify the causes of the differences between the residual drift ratios. It can also be noted that the differences between the correlations are not statistically significant. Table 5.1 summarizes the observations from the hypothesis tests.

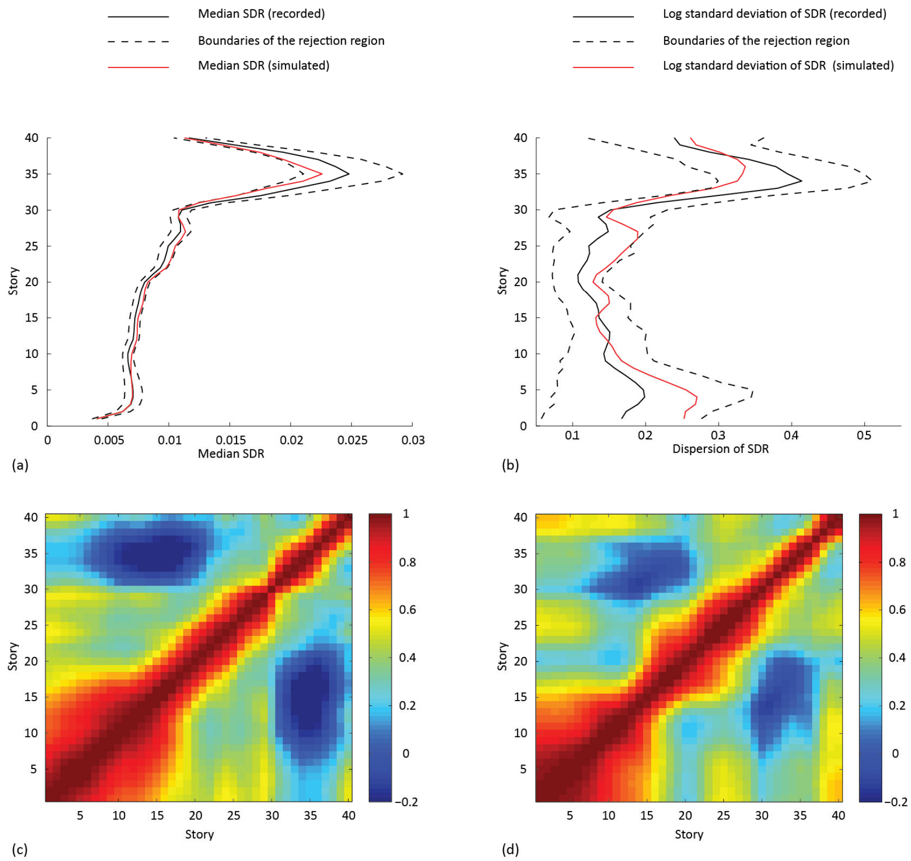

Figure 5.1. (a) Median SDR, (b) Dispersion of SDR, and story-story SDR correlation estimated using the selected (c) recorded and (d) simulated ground motions.

Table 5.1. Observations from the hypothesis tests

EDP	**Significance of deviation for**		
	Median	*Dispersion*	*Correlation*
SDR	Insignificant	Insignificant	Insignificant
PFA	Insignificant*	Insignificant	Insignificant
ResDR	Significant	Insignificant	Insignificant*
Moment	Insignificant	Insignificant	Insignificant
Rotation	Insignificant	Insignificant	Insignificant

Insignificant* denotes that the difference was close to the bound, although insignificant

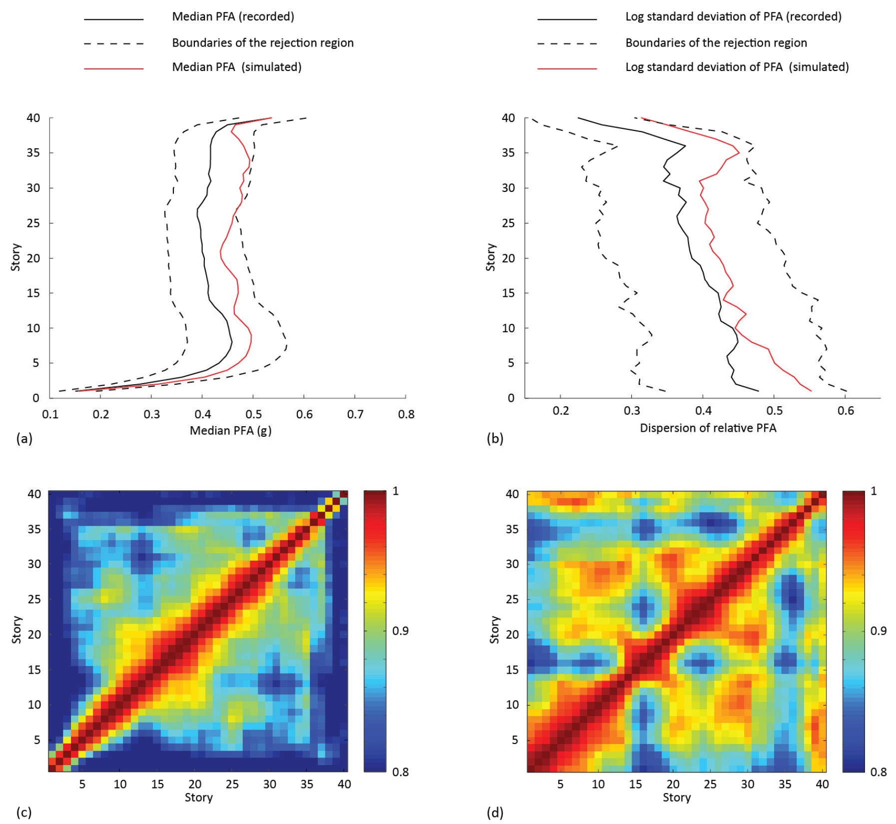

Figure 5.2. (a) Median PFA, (b) Dispersion of PFA.

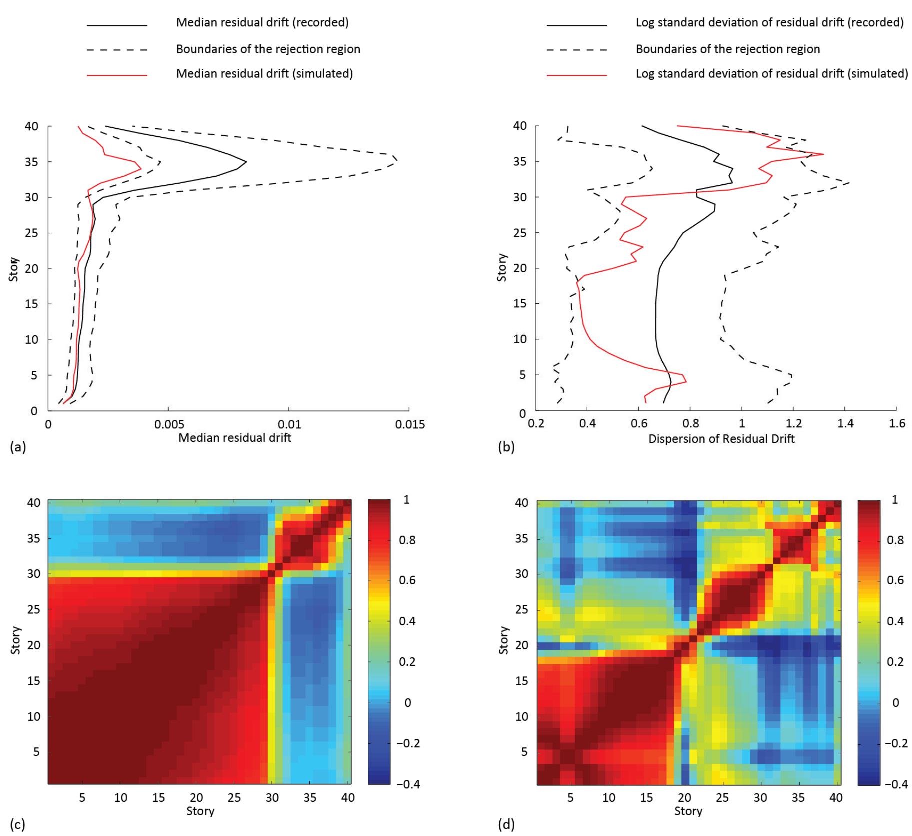

Figure 5.3. (a) Median residual drift, (b) Dispersion of residual drift.

5. CONCLUSIONS

This study illustrated a statistical approach to evaluate the level of similarity between the response of tall buildings to comparable recorded and simulated ground motions. Structural response measures of a 40 story steel moment frame building designed based on the 2006 IBC were estimated under 40 recorded and simulated ground motions selected from the NGA database and the 2009 broadband Loma Prieta simulations by Dr. Rob Graves. The ground motions were selected such that the mean and the variance of their spectra match a pre-specified target mean and variance. In order to ensure that the recorded and simulated ground motions are comparable, it was made sure that for each recorded ground motion, a simulated ground motion is selected so that the response spectra of both ground motions match. Additional constraints were imposed on the magnitudes, distances and the durations corresponding to the selected ground motions. The response measures considered were peak story drift ratio, peak floor acceleration, beam plastic rotation and residual drift ratio - measures that are commonly used to assess building performance while performing loss assessments. Hypothesis testing was then used to compare and contrast the response measures obtained using the selected recorded and simulated ground motions. The results of the study indicated that most response measures estimated using recorded and simulated ground motions are similar to each other. The one exception was the residual drift ratio, but additional research is necessary to identify the source of the difference. A similar study using the Puente Hills simulated records (Graves and Somerville 2006) for the same 40-story building (SCEC 2010) also produced similar conclusions. Overall, this study provided a statistical basis to test simulated ground motions and identify applications where simulated ground motions can be used.

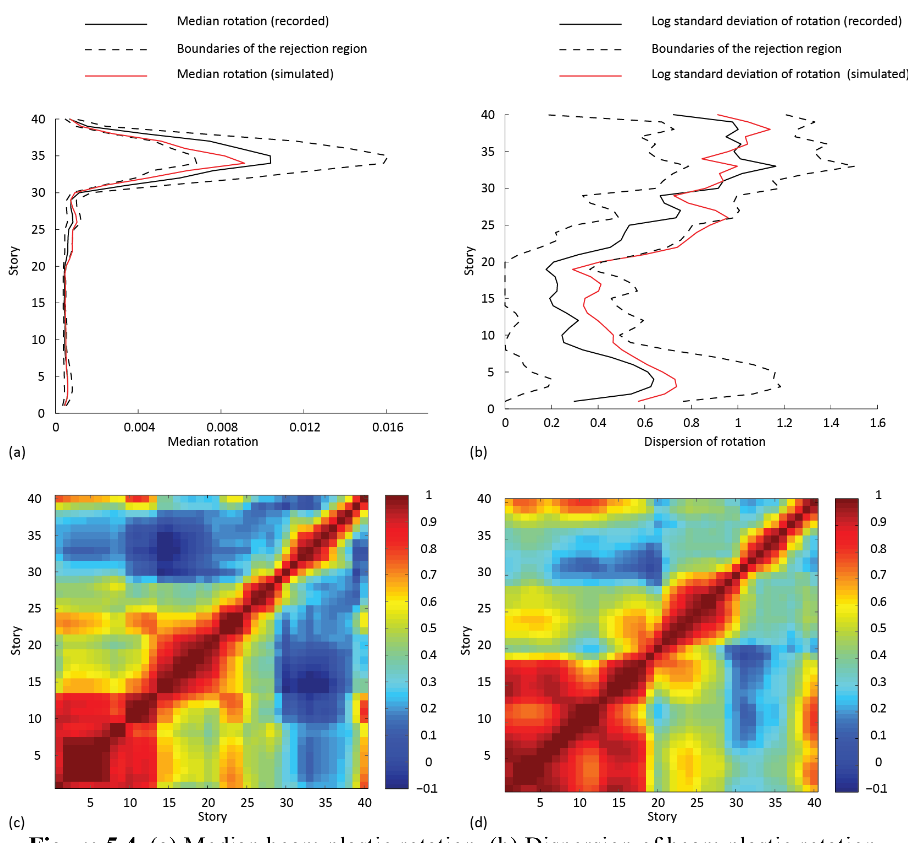

Figure 5.4. (a) Median beam plastic rotation, (b) Dispersion of beam plastic rotation.

REFERENCES

Aagaard, B.T., Brocher, D., Dolenc, D., Dreger, D., Graves, R.W., Harmsen, S., Hartzell, S., Larsen, S., and Zoback, M.L. (2008). Ground-motion modeling of the 1906 San Francisco earthquake, part 1: Validation using the 1989 Loma Prieta earthquake. *Bulletin of the Seismological Society of America* **98:2**,989-1011.

ATC-72 (2010). Modeling and Acceptance Criteria for Seismic Design and Analysis of Tall Buildings, Applied Technology Council.

Baker, J.W. (2011). The conditional mean spectrum: A tool for ground-motion selection. *Journal of Structural Engineering* **137:3**,322-331.

Baker, J.W. and Jayaram, N. (2008). Correlation of spectral acceleration values from NGA ground-motion models. *Earthquake Spectra* **24:1**,299-317.

Chiou, B.S.J., Darragh, R.B., Gregor, N.J. and Silva, W.J. (2008). NGA project strong motion database. *Earthquake Spectra* **24:1**,23-44.

Efron, B. And Tibshirani, R. (1993). An Introduction for the Bootstrap, Chapman & Hall/CRC.

Graves, R.W. and Somerville, P.G. (2006). Broadband Ground Motion Simulations for Scenario Earthquakes on the Puente Hills fault. Proceedings of *The Eighth National Conference on Earthquake Engineering*, San Francisco, CA. Paper No. 1052, Earthquake Engineering Research Institute.

Jayaram, N., and Baker, J.W. (2011). Statistical tests of the joint distribution of spectral acceleration values. *Bulletin of the Seismological Society of America* **98:5**,2231-2243.

Jayaram, N., Lin, T. and Baker, J.W. (2011). A computationally efficient ground-motion selection algorithm for matching a target response spectrum mean and variance. *Earthquake Spectra* **27:3**,797-815.

Jayaram, N., Shome, N. and Rahnama, M. (2011). Development of earthquake vulnerability functions for tall buildings. *Earthquake Engineering and Structural Dynamics*, in review.

Kutner, M.H., Nachtsheim, C.J., Neter, J., and Li, W. (2005). Applied Linear Statistical Models, The McGraw-Hill Companies Inc., New York, USA.

Lignos, D., and Krawinkler, H. (2009). Sidesway collapse of deteriorating structural systems under seismic excitations, *The John A. Blume Earthquake Engineering Center, Stanford University, Stanford, CA*. Rep. No. TB 172.

Luco, N., and Somerville, P., (2011). SCEC ground motion simulation validation workship, http://www.scec.org/workshops/2011/gmsv/index.html (last verified, March 2012).

Moehle, J., Bozorgnia, Y., Jayaram, N., Jones, P., Rahnama, M., Shome, N., Tuna, Z., Wallace, J., Yang, T., and Zareian, F. (2011). Case studies of the seismic performance of tall buildings designed by alternative means, *Task 12 Report for the Tall Buildings Initiative, Pacific Earthquake Engineering Research Center, CA*. Rep. No. 2011/05.

SCEC (2010). Do simulated and recorded time histories produce different building responses?-yes: Farzin Zareian/ no: Nirmal Jayaram / Nilesh Shome. *2010 SCEC Annual Meeting: Engineering Workshop on Tall Building Safety, Southern California Earthquake Center, Los Angeles, CA*.

USGS (2008). 2008 Interactive Deaggregations (Beta), https://geohazards.usgs.gov/deaggint/2008/ (last verified March, 2012).